01 Jul 2009

Near-Field Millimeter-Wave Imaging of Exposed and Covered Fatigue Cracks

Sergey Kharkovsky
Missouri University of Science and Technology

Mohammad Tayeb Ahmad Ghasr
Missouri University of Science and Technology, mtg7w6@mst.edu

R. Zoughi
Missouri University of Science and Technology, zoughi@mst.edu

Recommended Citation

S. Kharkovsky et al., "Near-Field Millimeter-Wave Imaging of Exposed and Covered Fatigue Cracks," *IEEE Transactions on Instrumentation and Measurement*, vol. 58, no. 7, pp. 2367-2370, Institute of Electrical and Electronics Engineers (IEEE), Jul 2009.
The definitive version is available at https://doi.org/10.1109/TIM.2009.2022380

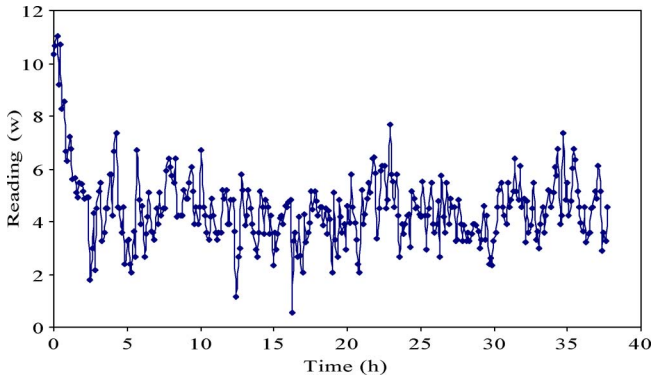

Fig. 2. Calibration of the zero power point.

calibration tests are conducted by controlling the input dc powers from 0 to 10 kW. The measured power losses from the calorimeter are all within a 0.2% accuracy. The experimental results for the zero point are shown in Fig. 2. Through analysis of these results, it can be observed that the calorimeter has a zero-point drift of approximately 5 W with a standard deviation of approximately 2 W.

The measurement errors identified in calibration tests have been input to the control program of LabView and will be compensated in the subsequent motor tests.

V. Conclusion

Calorimetry has long been acknowledged as an accurate tool for the measurement of power loss. Unfortunately, the previous calorimeters in the literature were all low-power facilities and achieved only limited success.

This paper has described the design of a 300-kW high-precision calorimeter. Refined from the two previous generations, this calorimeter is of air-cooled open type with improvements on heat leakage prevention and reduction in the test duration. This facility is capable of measuring power loss in electrical machines rated up to 300 kW with an overall accuracy of 0.2%. The power loss results from initial calibrations have confirmed the effectiveness and accuracy of the calorimeter.

Acknowledgment

The authors would like to thank Prof. G. M. Asher of Nottingham University, Nottingham, U.K., for his contribution on the preparation of this paper.

References

[1] U.S. Act, *The Energy Policy Act of 1992 (EPAct)*.
[2] CEMEP, *Voluntary Agreement for Minimum Standards for Electric Motors*. European Committee of Manufacturers of Electrical Motors and Power Electronics.
[3] *IEEE Standard Test Procedure for Polyphase Induction Motors and Generators (ANSI)*, IEEE Std. 112-2004 (IEEE 112-1991), 1996.
[4] K. J. Bradley, W. Cao, and J. Arellano-Padilla, "Evaluation of stray load loss in induction motors with a comparison of input-output and calorimetric methods," *IEEE Trans. Energy Convers.*, vol. 21, no. 3, pp. 682–689, Sep. 2006.
[5] *Rotating Electrical Motors—Part 2-1: Standard Methods for Determining Losses and Efficiency From Tests (Excluding Motors for Traction Vehicles)*, IEC 60034-2-1 (BS EN 60034-2-1), 2007.
[6] R. F. Clark, "A coaxial calorimeter for use as a microwave power standard," *IEEE Trans. Instrum. Meas.*, vol. IM-14, no. 1, pp. 59–63, Mar. 1965.
[7] N. P. Abbott, C. J. Reeves, and G. R. Orford, "A new waveguide flow calorimeter for levels of 1-20 W," *IEEE Trans. Instrum. Meas.*, vol. IM-23, no. 4, pp. 414–420, Dec. 1974.
[8] B. Vowinkel, "Broad-band calorimeter for precision measurement of millimeter- and submillimeter-wave power," *IEEE Trans. Instrum. Meas.*, vol. 29, no. 3, pp. 183–189, Sep. 1980.
[9] D. R. Turner, K. J. Binns, B. N. Shamsadeen, and D. F. Warne, "Accurate measurement of induction motor losses using balance calorimeter," *Proc. Inst. Elect. Eng.—Elect. Power Appl.*, vol. 138, no. 5, pp. 233–242, Sep. 1991.
[10] B. Baholo, P. H. Mellor, D. Howe, and T. S. Birch, "An automated calorimetric method of loss measurement in electrical motors," *J. Magn. Magn. Mater.*, vol. 133, pp. 433–436, 1994.
[11] D. J. Patterson, "An efficiency optimized controller for a brushless DC motor and loss measurement using a simple calorimetric technique," in *Proc. PESC*, 1995, vol. 1, pp. 22–27.
[12] O. Aglen, "Calorimetric measurement of losses in air cooled and water cooled asynchronous motors," in *ICEM*, Vigo, Spain, 1996, vol. 3, pp. 256–262.
[13] P. D. Malliband, D. R. H. Carter, B. M. Gordon, and R. McMahon, "Design of a double-jacketed, closed calorimeter for direct measurement of motor losses," in *7th Int. Conf. Power Electron. Variable Speed Drive*, Sep. 21–23, 1998, pp. 212–217.
[14] A. Jalilian, V. J. Gosbell, B. S. P. Perera, and P. Cooper, "Double chamber calorimeter (DCC): A new approach to measure induction motor harmonic losses," *IEEE Trans. Energy Convers.*, vol. 14, no. 3, pp. 680–685, Sep. 1999.
[15] B. Szabados and A. Mihalcea, "Design and implementation of a calorimetric measurement facility for determining losses in electrical motors," *IEEE Trans. Instrum. Meas.*, vol. 51, no. 5, pp. 902–907, Oct. 2002.
[16] E. Ritchie, J. K. Pedersen, F. Blaabjerg, and P. Hansen, "Calorimetric measuring systems," *IEEE Ind. Appl. Mag.*, vol. 10, no. 3, pp. 70–78, May/Jun. 2004.
[17] P. McLeod, K. J. Bradley, A. Ferrah, R. Magill, J. C. Clare, P. Wheeler, and P. Sewell, "High precision calorimetry for the measurement of the efficiency of induction motors," in *Conf. Rec. IEEE IAS Annu. Meeting*, Oct. 12–15, 1998, vol. 1, pp. 304–311.
[18] W. Cao, K. J. Bradley, and A. Ferrah, "Development of a high-precision calorimeter for measuring power loss in electrical motors," *IEEE Trans. Instrum. Meas.*, vol. 58, no. 3, pp. 570–577, Mar. 2009.

Near-Field Millimeter-Wave Imaging of Exposed and Covered Fatigue Cracks

Sergey Kharkovsky, *Senior Member, IEEE*, Mohammad T. Ghasr, *Student Member, IEEE*, and Reza Zoughi, *Fellow, IEEE*

***Abstract*—In this paper, the efficacy of near-field millimeter-wave nondestructive techniques, using open-ended flange-mounted rectangular waveguide probes, for extracting information of 3-D crack area deformation (i.e., in-plane and out-of-plane deformation) is demonstrated. It is shown that this information can be obtained from indications of unique interference patterns that are generated between the probe and the metal surface during the raster scan of a surface-breaking exposed and covered fatigue crack using a phase-sensitive reflectometer.**

***Index Terms*—Crack, imaging, interference pattern, millimeter waves, near field, nondestructive, reflectometer.**

Manuscript received March 2, 2009; revised April 28, 2009. First published May 19, 2009; current version published June 10, 2009. The Associate Editor coordinating the review process for this paper was Dr. Wendy Van Moer.

The authors are with the Applied Microwave Nondestructive Testing Laboratory, Department of Electrical and Computer Engineering, Missouri University of Science and Technology, Rolla, MO 65409 USA (e-mail: sergiy@mst.edu; mtg7w6@mst.edu; zoughir@mst.edu).

Digital Object Identifier 10.1109/TIM.2009.2022380

I. Introduction

Once a surface-breaking fatigue crack appears in a metal structure, evaluating its 3-D (i.e., in-plane and out-of-plane) area deformation characteristics becomes critical [1]. Standard nondestructive inspection (NDI) methods used for this purpose primarily provide in-plane crack area deformation information (i.e., detection and evaluation of a crack opening), while only a few methods such as a combined optical Moire–Sagnac interferometry [1] have successfully been used to measure the 3-D crack area deformation characteristics. However, these techniques are complex, require bulky instrumentation, and have a problem with the evaluation of cracks in metals covered with an optically opaque dielectric coating. Since the mid 1990s, near-field microwave and millimeter-wave techniques have demonstrated their capability for detecting surface-breaking fatigue cracks and evaluating their various properties [2]–[4]. These techniques have certain distinct advantages over the other "standard" NDI techniques when detecting and evaluating cracks in exposed and covered cracks. In addition, they are fast, reliable, and relatively inexpensive techniques. However, thus far, the primary attention has been focused on obtaining reliable in-plane measurement information. This paper presents the operational principles of a near-field millimeter-wave imaging technique, utilizing a flange-mounted rectangular waveguide probe and a phase-sensitive reflectometer, for exposed and covered fatigue crack detection while demonstrating the potential of this technique for analyzing the 3-D surface deformation immediately around the crack region.

II. Measurement Approach

Fig. 1 shows a measurement setup with an open-ended flange-mounted rectangular waveguide probe held above a metal plate with a surface crack at a certain distance d (referred to as the standoff distance). To detect a surface-breaking fatigue crack, the incident electric field polarization vector must be perpendicular to the long axis of the crack or its length (i.e., the perpendicular polarization) [2]. Electromagnetically, a surface discontinuity such as a crack in a metal plate disturbs the induced surface current density and significantly alters the resulting reflected wave compared to that when there is no crack present [2]. In the combined flange-mounted waveguide and metal surface structure shown in Fig. 1, the near field of the probe constitutes the area under the waveguide aperture and that under the flange. In previous investigations, perturbations in the form of additional peaks near the edges of the flange in the measured crack characteristic signal (i.e., detected signal as a function of scanning distance over a crack) were observed [3], [4]. The source of these perturbations is found to be the guided waves between the metal surface and the flange and the waves reflected by discontinuities in this guiding structure (e.g., edges of the flange). The presence of a crack under the flange also changes the properties of these waves, and at millimeter-wave frequencies, the combination of all of these reflected waves manifests itself as an interference pattern [2] (as the waveguide scans the crack) since the side dimension of a standard flange is comparable with a wavelength at these frequencies. It will be shown in this paper that this pattern provides information about in-plane and out-of-plane crack area deformations such as a displacement between crack edges, which causes a change in the standoff distance on either side of the crack, as indicated by distance d_1 in Fig. 1. The presence of these changes primarily influences the phase and, to a lesser degree, the magnitude of the reflected signal. To investigate these changes, a (primarily) phase-sensitive reflectometer may be employed. To this end, a millimeter-wave reflectometer similar to that used in [3] was used for this investigation, as shown in Fig. 1. This reflectometer

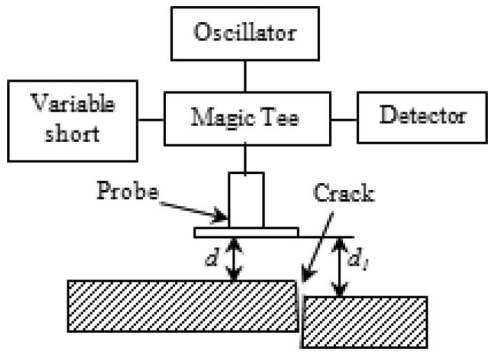

Fig. 1. Schematic (not to scale) of a setup with an open-ended flange-mounted waveguide probe testing the sample with a surface crack with out-of-plane displacement.

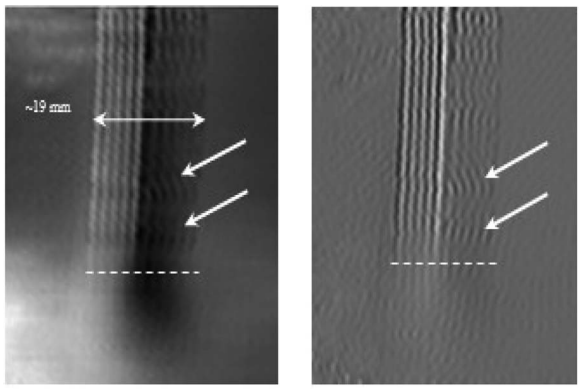

(a) (b)

Fig. 2. (a) Two-dimensional image of the crack obtained at d∼0.2 mm and at 90 GHz. (b) Two-dimensional processed image after horizontal gradient filtering.

possesses at least two important attractive features: 1) sensitivity to the changes in both the phase and magnitude of the reflected signal and 2) the availability of a phase-adjustable reference signal via a variable short, by which detection sensitivity may be enhanced and optimized.

In this investigation, the metal plate was placed on a computer-controlled scanning table, while the probe was held at a fixed position above the plate. As the scanning table moved the plate under the probe, a 2-D matrix consisting of dc voltages proportional to the local reflection properties of the plate was produced and recorded. The 2-D image produced in this way provides information about relative signal variation in and around the crack region.

III. Results and Discussion

Several plates containing surface-breaking fatigue cracks were investigated at W-band (frequency range of 75–110 GHz with corresponding free-space wavelength λ from 4–2.7 mm). One of the plates was a section of a 12-mm-thick A-36 steel sample with a few through fatigue cracks (i.e., crack depth equal to the metal sample thickness) created by cyclical loading [4]. A W-band open-ended flange-mounted rectangular waveguide probe with an aperture dimension of 2.54 mm × 1.27 mm and with a square (19 mm × 19 mm) flange was used in this investigation.

Fig. 2(a) shows a 90-GHz 2-D image of a 50 mm × 70 mm area around one of the cracks with an opening of ∼0.005–0 mm along its length, obtained at a standoff distance of d∼0.2 mm. Several

observations can be made from the 2-D image [Fig. 2(a)]. The indication of the crack can be seen in the middle of the image, which is surrounded by a series of dark and bright lines (i.e., interference pattern) on either side of it. The total extent of these interference patterns corresponds to the dimension of the flange ($\sim$19 mm), as shown in Fig. 2(a) by the solid line (arrowed). It must be noted that a previous careful inspection of the metal plate showed that it had a tiny displacement (out-of-plane deformation) between the left and right edges of the crack ranging from $\sim$0.02 to 0 mm along the crack. This crack edge displacement is indicated by the intensity contrast between the regions to the left and to the right of the crack in the image. The average voltage difference on either side of the crack is $\sim$40 mV, which is substantial and can readily be measured. The interference patterns are also distorted in some places, particularly on the right side marked by arrows in Fig. 2(a), which indicates the nonuniformities associated with the crack edges. In addition, the indication of the interference patterns provides information about the crack length, which leads to the critically important information about the exact location of the crack tip. Fig. 2(a) shows that there are no indications of the crack and the interference patterns in the region below the dashed line that passes through the crack tip. On the other hand, the intensity contrast between the left and right sides of the crack (indicating the out-of-plane deformation) extends below this line.

In applications involving crack sizing, it may be necessary to remove or reduce the influence of the displacement and/or the interference patterns on the produced image. Reducing the influence of the displacement indication may be accomplished applying a relatively simple gradient filter [5] to the image. For instance, Fig. 2(b) shows the processed image using a horizontal gradient filter. The processed image [Fig. 2(b)] clearly shows enhanced indication of the crack and the interference patterns, including the nonuniformities in the interference pattern due to crack edges. The intensity contrast between the left and right sides of the crack indication is still somewhat visible in this image, but it is much less pronounced than that shown in Fig. 2(a), as expected. Furthermore, the crack tip is clearly visible in this processed image, while the gradient filter essentially removed the indication of the out-of-plane deformation in the region below the crack tip (marked by the dashed line).

The results of crack imaging at a relatively wide range of standoff distances $(0 < d < 2\lambda)$ showed that when the standoff distance increases, the indication of the interference patterns gradually decreases. For instance, Fig. 3(a) shows a 2-D image of the crack obtained at a standoff distance of $d\sim$1.7 mm, while the indications of the interference patterns are much less pronounced than those shown in Fig. 2(a). The 2-D image shown in Fig. 3(a) provides comprehensive information about the entire crack and the 3-D deformation around the crack, including the crack tip location, nonuniformities associated with the crack edges, and the deformation below the tip marked by the dashed arrow.

The indication of the crack is more prominent in this image than in the image at $d\sim$0.2 mm [Fig. 2(a)]. This is due to the fact that the indications of the displacement and the interference patterns are less pronounced in this image. This fact can clearly be seen in the 1-D profile as shown in Fig. 3(b), which is a linear scan across the 2-D image, as shown in Fig. 3(a) by a horizontal dark line. Another important observation in Fig. 3(b) is that there is an obvious average voltage difference on either side of this 1-D profile. This voltage difference is due to the relative out-of-plane displacement between the edges of the crack, as mentioned earlier. In Fig. 3(b), this voltage difference is $\sim$25 mV, which is less than that for $d\sim$0.2 mm (mentioned earlier to be $\sim$40 mV) but is still substantial and can readily be measured.

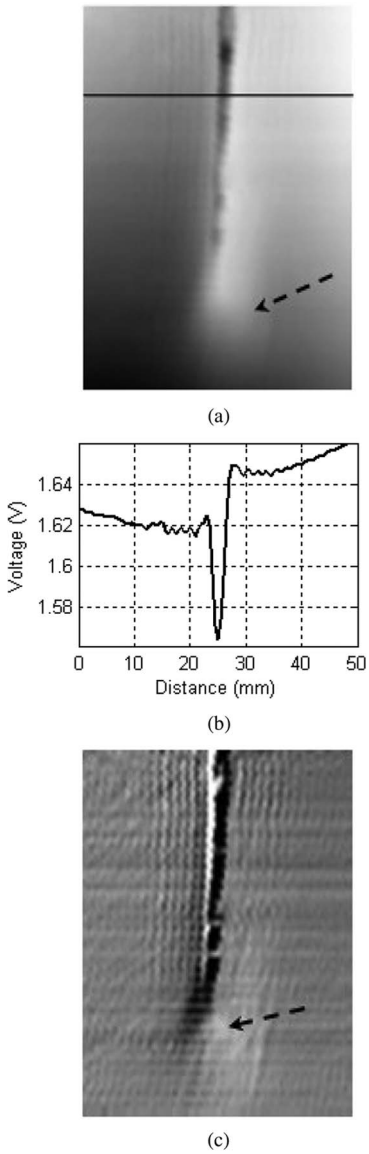

Fig. 3. (a) Two-dimensional image of the crack obtained at $d\sim$1.7 mm. (b) One-dimensional profile of the crack. (c) Two-dimensional processed image after horizontal and vertical gradient filtering.

The 2-D image was processed using horizontal and vertical gradient filtering, as shown in Fig. 3(c). This resulted in a sharper crack indication, including its tip location, nonuniformities in the crack geometry, and the deformation below the tip marked by the dashed arrow. The indication of the interference patterns was enhanced as well, but it was much less pronounced compared to the enhancement in the crack image. In addition, Fig. 3(c) shows that the two interference patterns are not the same, indicating the influence of the relative standoff distance change during the scan and, hence, the presence of out-of-plane deformation.

The detection and evaluation of cracks under thin dielectric coatings such as paint was also successfully conducted with this technique. Fig. 4 shows the 1-D profile and the 2-D image of the portion of the crack covered by a 0.2-mm-thick piece of tape (possessing dielectric properties similar to those of common paint) and at a standoff distance of $d\sim$1.7 mm. Comparing the 1-D profiles and the 2-D images of the exposed crack at the same standoff distance (i.e., Fig. 3) with those shown in Fig. 4 with the same location of 1-D profile shows that the indication of the covered crack is somewhat less pronounced, while

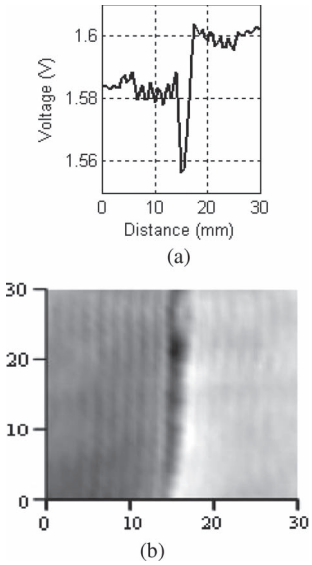

Fig. 4. (a) One-dimensional profile and (b) two-dimensional image of the portion of covered crack obtained at $d\sim$1.7 mm (scanned area of 30 mm $\times$ 30 mm).

the indications of the interference patterns in the 1-D profiles are more pronounced in Fig. 4(a) than in Fig. 3(b). These observations show that both phase and magnitude changes contributed to the indication changes due to the tape.

IV. Conclusion

The near-field millimeter-wave imaging technique, as has been described in this paper, is capable of providing useful information about the presence and properties of a tight surface-breaking exposed and covered fatigue crack in metals. The efficacy of this technique for 3-D crack area surface deformation measurement, including the measurement of the extent of crack tip deformation region, was also demonstrated. The method is fast, nondestructive, easy to perform, simple, inexpensive, and conducive for online and real-time applications while requiring little to no signal processing and operator expertise.

References

[1] B. S.-J. Kang and S. M. Anderson, "Three-dimensional crack tip deformation measurement using combined Moire-Sagnac interferometry," *Exp. Mech.*, vol. 41, no. 1, pp. 84–91, Mar. 2001.

[2] R. Zoughi and S. Kharkovsky, "Microwave and millimeter wave sensors for crack detection," *Fatigue Fract. Eng. Mater. Struct.*, vol. 31, no. 8, pp. 695–713, Aug. 2008.

[3] N. Qaddoumi, E. Ranu, and R. Zoughi, "Microwave detection of stress-induced fatigue cracks in steel and potential of crack opening determination using a new phase sensitive approach based on a waveguide magic tee," in *Review of Progress in Quantitative Nondestructice Evaluation*, vol. 18A, D. O. Thompson and D. E. Chimenti, Eds. New York: Kluwer, 1999, pp. 569–576.

[4] N. Qaddoumi, E. Ranu, J. D. McColskey, R. Mirshahi, and R. Zoughi, "Microwave detection of stress-induced fatigue cracks in steel and potential for crack opening determination," *Res. Nondestruct. Eval.*, vol. 12, no. 2, pp. 87–103, Oct. 2000.

[5] A. K. Jain, *Fundamentals of Digital Image Processing*. Englewood Cliffs, NJ: Prentice-Hall, 1989, pp. 348–350.